Mon. Not. R. Astron. Soc. **270,** L17–L21 (1994)

The unified Seyfert scheme and the origin of the cosmic X-ray background

Piero Madau,[1] Gabriele Ghisellini[2] and A. C. Fabian[3]

[1] *Space Telescope Science Institute, 3700 San Martin Drive, Baltimore, MD 21218, USA*
[2] *Osservatorio Astronomico di Torino, Strada Osservatorio 20, I-10025 Pino Torinese, Italy*
[3] *Institute of Astronomy, Madingley Road, Cambridge CB3 0HA*

Accepted 1994 June 24. Received 1994 June 24; in original form 1994 June 13

ABSTRACT

We discuss a simple model for the cosmic X-ray background (XRB), based on the unified Seyfert scheme. We show that a mixture of unabsorbed type 1 and absorbed type 2 Seyferts, integrated in redshift back to $z = 3.5$, can simultaneously reproduce the spectrum of the XRB from 1 to 150 keV and the source counts in both the soft and hard X-ray bands. The presence of numerous, heavily obscured sources with hard spectra at a flux level of 10^{-12} erg cm^{-2} s^{-1} is indicated as a test of the model, in view of forthcoming *ASCA* observations.

Key words: quasars: general – galaxies: Seyfert – diffuse radiation – X-rays: galaxies.

1 INTRODUCTION

According to the unified Seyfert scheme (Antonucci & Miller 1985; Miller & Goodrich 1990; Antonucci 1993), obscuring matter, probably having toroidal geometry and at a distance of several parsecs from the central powerhouse, blocks our line of sight to the nucleus of a Seyfert galaxy. When we view the object along the axis, we see a Seyfert 1; when our view is occulted by the torus, photons of all energies from the far-infrared to several keV are blocked, and in these bands we can only detect the nucleus indirectly. We then see a Seyfert 2. The unified Seyfert scheme predicts the existence of many heavily obscured sources, the X-ray spectra of which are reprocessed by photoelectric absorption and scattering in cold, possibly Compton-thick material. The obscuration hypothesis is supported by X-ray studies of Seyfert galaxies. Type 1 Seyferts are known to emit nearly as much energy in the X-ray band as anywhere else in the spectrum, while most type 2 Seyferts are weak in X-rays, particularly at a few keV (e.g. Awaki et al. 1991). In a UV-selected sample of type 2 Seyferts observed with *Ginga*, Mulchaey, Mushotzky & Weaver (1992) found absorbing column densities ranging from 3×10^{22} cm^{-2} to $>10^{24}$ cm^{-2}. Because many type 2 Seyferts were not detected by *Ginga* (Awaki 1992), it is likely that the obscuring torus in these cases is optically thick to Compton scattering, i.e. $N_{\rm H}>$ a few $\times10^{24}$ cm^{-2}.

The impact of the unified Seyfert scheme on the estimated contribution of low-luminosity active galactic nuclei (AGNs) to the XRB is two-fold. First, since Seyfert 1 galaxies produce at least 20 per cent of the XRB in the 2–10 keV band (Piccinotti et al. 1982) and the inferred covering factor of the obscuring torus is large, the Seyfert galaxy population as a whole should contribute substantially to the XRB. Secondly, heavy photoelectric absorption would reprocess the intrinsic spectrum below ~20 keV. Setti & Woltjer (1989) first suggested that a population of obscured, weakly evolving Seyfert 2 galaxies could indeed account for the flat XRB spectrum in the 3–20 keV interval (see also Morisawa et al. 1990; Grindlay & Luke 1990). A high density of absorbed sources is also suggested by a comparison between the number counts in the soft and hard X-ray bands (see e.g. Stewart 1992; Butcher et al. 1994).

The scenario in which a large fraction of the XRB is produced by a mixture of absorbed Seyfert 2 and unabsorbed Seyfert 1 galaxies is then a direct consequence of the unified Seyfert scheme. In a previous paper (Madau, Ghisellini & Fabian 1993, hereafter Paper I), we performed a preliminary investigation of the X-ray spectral properties of obscured AGNs. We considered the reprocessing of X-rays in cold thick material, and computed the transmitted spectra expected for type 2 Seyferts. We pointed out the general features of a simple obscuration model, showing that the integrated contribution from Seyfert galaxies can provide a good fit to the XRB if the blocking material has Thomson depth $\tau_{\rm T}\sim1$ and a large covering factor.

Using the known cosmological evolution of the AGN X-ray luminosity function, we show in this Letter that a simple model based on the unified Seyfert scheme is able simultaneously to reproduce the spectrum of the XRB and the source counts in both the soft and hard X-ray spectral domains, and makes definite predictions about the density of

heavily absorbed AGNs which can be tested by *ASCA* observations. A somewhat similar model has been outlined by Comastri et al. (1994).

2 MODEL DEFINITION AND CALCULATION

2.1 Type 2 to type 1 Seyfert number ratio

The ratio of obscured to unobscured solid angle can be estimated by counting the number of type 2 objects relative to type 1. Efforts to date indicate that the integrated space density of Seyfert 2 galaxies is between 2 and 10 times larger than the density of Seyfert 1 galaxies (Phillips, Charles & Baldwin 1983; Osterbrock & Shaw 1988; Huchra & Burg 1992).

2.2 Cosmological evolution of X-ray-selected AGNs

According to Boyle et al. (1993), who have combined survey results from *ROSAT* (Shanks et al. 1991) and *Einstein* (Della Ceca et al. 1992), the model that best fits the cosmological evolution of X-ray-selected AGNs in an Einstein–de Sitter, $q_0 = 0.5$ universe is one in which the comoving volume emissivity increases as $(1+z)^k$ for $z \lesssim z_c$, with $k = 2.5 \pm 0.1$ and $z_c = 2$, and remains constant for $z_c < z \lesssim z_{max}$, with $z_{max} \sim 3.5$, in qualitative agreement with the evolution of the QSO optical luminosity function (Boyle 1991; Zitelli et al. 1992).

2.3 The X-ray background

The XRB spectrum is characterized by a narrow peak in spectral power, EI_E, at 30 keV; a simple analytical fit from 3 to 60 keV yields $I_E \simeq 7.7 E_{keV}^{-0.29} \exp(-E_{keV}/40)$ keV cm^{-2} s^{-1} sr^{-1} keV^{-1} (Boldt 1987). Until recently, the soft X-ray background below 3 keV, as seen by *Einstein* and *ROSAT*, appeared to be a distinct, steeper component (Wu et al. 1990; Hasinger, Schmidt & Trümper 1991). Initial results from the *ASCA* satellite have instead shown that a single power law with energy index ~ 0.4 describes well the XRB in the 1–10 keV band, with no evidence for steepening in the 1–3 keV range (Gendreau et al. 1994).

2.4 X-ray properties of Seyfert galaxies

In the 2–10 keV band, the X-ray spectrum of type 1 Seyferts is well fitted by a power law with energy index $\alpha = 0.7 \pm 0.17$ (Turner & Pounds 1989), too steep to match the XRB. *Ginga* observations of Seyfert 1 galaxies in the 2–30 keV band (Pounds et al. 1990; Matsuoka et al. 1990) have shown the presence of a flat component above 10 keV. Along with the iron K-fluorescent line, this feature can be explained either by reflection of an incident power law from cold gas close to the central compact object, e.g. an accretion disc (Pounds et al. 1990), or by reprocessing from a more distant obscuring torus (Krolik, Madau & Życki 1994; Ghisellini, Haardt & Matt 1994).

To date, only a few AGN spectra have been measured in the hard X-ray band. The OSSE instrument on-board *GRO* has observed a sharp cut-off in the spectrum of NGC 4151, with an e-folding energy of 50 keV (Maisack et al. 1993). The observed energy distribution of IC 4329A is instead compatible with an e-folding energy of $\gtrsim 200$ keV (Madejski et al. 1994). Although not established for all Seyferts (Johnson et al. 1994), this spectral form is suggestive of a thermal electron distribution which might account for the hard XRB break. Note that thermal plasmas in pair equilibrium (Svensson 1984) might act as a thermostat, giving rise to a preferred range of observed temperatures. The exact value of the limiting temperature depends mainly on the compactness of the source [defined as $\ell \equiv \sigma_T L/(m_e c^3 R)$, where L/R is the luminosity-to-size ratio]. For compactness parameters corresponding to a few per cent of the Eddington luminosity ($\ell \sim 100$), and $\alpha = 0.9$, the predicted plasma temperature is ~ 150 keV, which yields an e-folding energy of $300 \lesssim E_c \lesssim 450$ keV if thermal Comptonization of soft photons is the dominant radiation mechanism (Sunyaev & Titarchuk 1980).

2.5 Radiation transfer modelling

Following Paper I, we model the thick torus which covers most of the solid angle around the active nucleus as a homogeneous spherical cloud of cold material surrounding the central X-ray source. As in Paper I, the radiation transfer is computed with a Monte Carlo code constructed using the photon-escape weighting method of Pozdnyakov, Sobol' & Sunyaev (1983). More sophisticated codes able to cope with 2D geometry have been recently developed by Krolik et al. (1994) and Ghisellini et al. (1994). We set the electron temperature T_e equal to zero, and adopt the full Klein–Nishina scattering cross-section. The bound–free opacity associated with standard cosmic-abundance material is taken from Morrison & McCammon (1983). Each Monte Carlo run uses 5×10^5 input photons.

We assume for the primary flux a power law multiplied by an exponential:

$$I_E \propto E^{-\alpha} \exp\left(-\frac{E}{E_c}\right), \qquad (1)$$

with $\alpha = 0.9$ (Nandra & Pounds 1994) and $E_c = 360$ keV. These seed photons are Compton-reflected towards the observer by a semi-infinite cold disc close to the primary X-ray source. A fraction f of this radiation is directly observed and mimics the contribution of the unabsorbed Seyfert 1 population, while a fraction $1-f$ is further reprocessed by a thick absorbing torus. Following Huchra & Burg (1992), we set the number ratio of type 2 to type 1 Seyferts, $(1-f)/f$, equal to 2.5. The hydrogen column density of the obscuring material along the line of sight is taken to have a Gaussian distribution of $\log N_H$, with mean value equal to 24 and dispersion $\sigma = 0.8$. A small spectral component, equal to only 2 per cent of the primary incident power, is added to the transmitted Seyfert 2 spectra. This represents the flux scattered into the line of sight by electrons in the warm, ionized medium located above the axis of the obscuring torus (Miller, Goodrich & Mathews 1991). Finally, all spectra are filtered through a galactic absorbing column of 5×10^{20} cm^{-2}.

Fig. 1(a) plots the energy distributions of the individual type 1 and type 2 Seyferts which contribute to the XRB, according to our model. In type 1 objects the best-fitting spectral index is 0.78 in the 2–18 keV range, and 0.58 in the 10–18 keV range. In type 2 galaxies the emergent intensity per logarithmic energy interval forms a hump, whose position and width are determined by the competition between bound–free absorption at low energies, and Compton down-

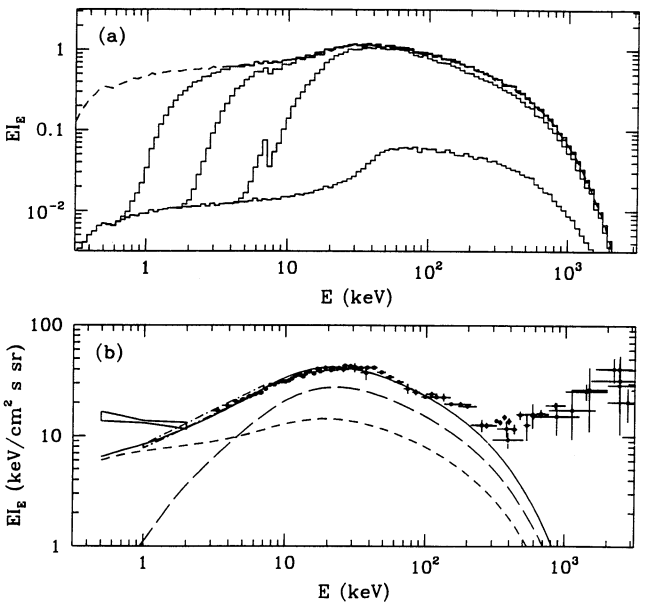

Figure 1. (a) The short-dashed line is the composite spectrum associated with type 1 Seyferts. This is the sum of a direct component of the form $I_E \propto E^{-\alpha}\exp(-E/E_c)$, with $\alpha=0.9$ and $E_c=360$ keV, plus a reflected component from a semi-infinite slab. The histograms are the transmitted type 2 spectra for $\log N_H=22.1$, 23.1, 24.1 and 25.1 (left to right), with 2 per cent of the primary incident power added to represent the flux scattered into the line of sight by electrons in the warm, ionized medium. All spectra are filtered through a galactic absorbing column of 5×10^{20} cm^{-2}. (b) XRB spectrum (solid curve) produced by a 2.5:1 mixture ($f=0.28$) of absorbed type 2 (long-dashed line) and unabsorbed type 1 (short-dashed line) Seyferts, compared with the data. The obscuring torus is assumed to have a Gaussian distribution of $\log N_H$, with mean value equal to 24 and dispersion $\sigma=0.8$. The evolutionary parameters are $k=2.55$, $z_c=2$ and $z_{max}=3.5$, in a $q_0=0.5$ universe. The *ROSAT* soft XRB spectrum, shown by the elongated 0.5–2 keV (solid) error contour, is in disagreement with the *ASCA* recent measurements, shown by the elongated 1–7 keV (dot-dashed) error contour.

scattering and exponential roll-off of the injected spectrum at high energies. It is this hump which, with the right amount of cosmological evolution, provides a good fit to the XRB above 10 keV. Cold, thick matter along the line of sight will also produce an Fe Kα emission line. This feature will be smeared out in the XRB because of the cosmological evolution of the emitting sources (Matt & Fabian 1994).

2.6 Comparison with the data

Fig. 1(b) shows a comparison between the data and the predicted contribution of Seyfert galaxies to the background. Our simple model fits the XRB within 10 per cent from 1 to 150 keV. The normalization yields $\langle nL\rangle^0_{2-10}\simeq 4.7\times10^{38}\ h_{50}$ erg s^{-1} Mpc^{-3} ($h_{50}\equiv H_0/50$ km s^{-1} Mpc^{-1}) for the 2–10 keV emissivity at $z=0$, and $\langle nL\rangle^0_{0.3-3.5}\simeq 3.6\times10^{38}\ h_{50}$ erg s^{-1} Mpc^{-3} in the 0.3–3.5 keV energy band. The 2–10 keV emissivity is in very good agreement with that found by Miyaji et al. (1994) from cross-correlating *IRAS* galaxies and the XRB intensity observed with *HEAO-1*. While the dominant contribution to the observed intensity below 3 keV comes from type 1 Seyferts, Seyfert 2 galaxies produce most of the hard XRB. The superposition of steep type 1 and absorbed type 2 X-ray spectra explains the flat slope of the 1–20 keV background. Note that, if the X-ray photon distribution of Seyfert galaxies breaks at much higher energies, say $E_c\sim1$ MeV, then their integrated contribution to the 2–10 keV flux cannot exceed 40 per cent in order not to overproduce the hard XRB.

3 X-RAY NUMBER COUNTS

An AGN model that fits the XRB spectrum should simultaneously be consistent with the observed sky density of sources as a function of X-ray limiting flux (the $\log N$–$\log S$ relationship). In this section we try to account for the source counts in both the soft and hard X-ray spectral domains in terms of a single AGN population. For our present purpose, we ignore the soft X-ray spectral excesses observed below 1 keV, and the likely presence of two separate, intrinsically soft and hard X-ray AGN populations (Comastri et al. 1992; Franceschini et al. 1993).

3.1 Luminosity function of AGNs

The present-epoch 0.5–2 and 2–10 keV emissivities computed from our model are comparable to the AGN emissivities in the same bands derived from the Piccinotti et al. (1982) and the Boyle et al. (1993) luminosity functions (LFs). For simplicity, we assume that the local LF of type 1 Seyferts in the 2–10 keV band is a single power law

$$n(L)=\frac{n_1}{L_1}\left(\frac{L}{L_1}\right)^{-2.75} \qquad (2)$$

for $L_1\le L\le L_2$, where $L_1=7\times10^{42}$ erg s^{-1}, $L_2=100L_1$ and $n_1=3.3\times10^{-5}$ Mpc^{-3}. The distribution of type 2 Seyferts that we derive can be approximated by a broken power law with break luminosity $L\sim L_1$. For $L>L_1$, Seyfert 1 outnumber Seyfert 2 galaxies by a factor of $\gtrsim3.5$. The sum of type 1 and type 2 AGNs is consistent with the observed 2–10 keV LF of Seyfert galaxies (Piccinotti et al. 1982; Persic et al. 1989).

3.2 Log N–log S relation

Although type 2 Seyferts are twice as numerous as type 1s, the reduction in their low-energy flux due to photoelectric absorption is such that sources of this type should be severely under-represented in soft X-ray surveys at all but the faintest fluxes. Their contribution to the source counts at higher energies should, however, be substantial. Figs 2(a) and (b) show a comparison between the predicted $\log N$–$\log S$ curve of Seyfert galaxies and the observed density of X-ray sources in the hard 2–10 keV band of the *HEAO-1* A2 survey (Piccinotti et al. 1982) and in the soft 0.5–2 keV *ROSAT* band (Hasinger et al. 1993). The agreement is fairly good. In particular, our model is able to reproduce the observed flattening of the *ROSAT* counts below a flux of 10^{-14} erg cm^{-2} s^{-1}. As type 2 Seyferts dominate the 0.5–2 keV source counts below 10^{-15} erg cm^{-2} s^{-1}, however, the predicted $\log N$–$\log S$ relation steepens again. Our model resolves 100 per cent of the 0.5–2 keV XRB observed by

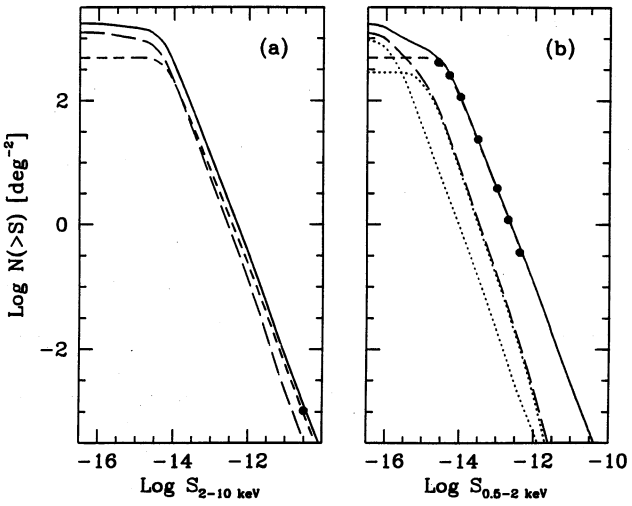

Figure 2. Total predicted number counts (solid curve), together with the Seyfert 1 (short-dashed line) and Seyfert 2 (long-dashed line) contributions. (a) 2–10 keV log N–log S relation with the Piccinotti et al. (1982) point indicated by the filled circle. (b) Predicted 0.5–2 keV log N–log S relation, compared with the *ROSAT* points (Hasinger et al. 1993). The two dotted curves depict type 2 Seyferts with log $N_H < 23.5$ (right) and > 23.5 (left). The total surface density of AGNs is ~ 2000 deg^{-2}.

ASCA at $S_{0.5-2} \sim 10^{-16}$ erg cm^{-2} s^{-1}. The total surface density of AGNs is ~ 2000 deg^{-2}. In the 2–10 keV band, the estimated ratio between type 1 and type 2 Seyferts is ~ 3 at $S_{2-10} = 3 \times 10^{-11}$ erg cm^{-2} s^{-1}, in agreement with the findings of Piccinotti et al. (1982).

4 SUMMARY

In this Letter we have presented a model for the XRB based on the unified Seyfert scheme. Much of the preceding material can be summarized as follows.

(1) A 1:2.5 mixture of unabsorbed type 1 and absorbed type 2 Seyferts, integrated in redshift according to the known cosmological evolution of the AGN X-ray LF, reproduces well the XRB spectrum from 1 to 150 keV. The primary photon distribution assumed for the individual sources is a steep power law with an exponential cut-off at 360 keV. Such a break is suggested by recent OSSE observations. With no high-energy cut-off, a population of evolving Seyfert galaxies would overproduce the hard XRB. We also note that it is difficult to fit the flat $\alpha \sim 0.4$ slope of the XRB observed in the 1–3 keV range without significant self-absorption. Models based on strongly enhanced Compton-reflected spectra (Fabian et al. 1990; Rogers & Field 1991; Terasawa 1991) and thermal Comptonization plus reflection spectra (Zdziarski, Życki & Krolik 1993) need strong evolution of the luminosity density up to $z \sim 8$ to reproduce the recent *ASCA* measurements. Here we have kept f and E_c independent of L, an assumption which we shall relax in later work. For the present, we note that good fits are obtained provided that $2.2 < k < 2.7$, $23.5 < \log N_H < 24$, $0.75 < \sigma < 1.6$, $2 < z_c$, $z_{max} < 3.5$, and 2 < type 2/type 1 < 3.

(2) Our model is able to provide a quantitative unified explanation of the results of several surveys in both the soft and hard X-ray bands. We fit the observed flattening of the *ROSAT* 0.5–2 keV log N–log S relation below 10^{-14} erg cm^{-2} s^{-1}, but predict a re-steepening of the source counts as heavily absorbed type 2 Seyferts start to dominate below 10^{-15} erg cm^{-2} s^{-1}. A re-steepening of the log N–log S curve below the *ROSAT* detection threshold has been observed in the optical source counts (Zitelli et al. 1992). In the 2–10 keV spectral domain, the contribution of type 2 Seyferts to the counts is significant even at the bright end. Type 1 still outnumber type 2 objects by a factor of ~ 3 at $S_{2-10} \sim 3 \times 10^{-11}$ erg cm^{-2} s^{-1}, as observed by Piccinotti et al. (1982). The surface densities of the two populations become comparable at $\sim 10^{-14}$ erg cm^{-2} s^{-1}.

The predicted number of obscured sources can also explain why the *ROSAT* soft X-ray source counts differ from the *Ginga* fluctuation analysis in the 2–10 keV band. At a flux level of $S_{2-10} \sim 10^{-13}$ erg cm^{-2} s^{-1}, a conversion factor appropriate for the $\alpha \sim 1$ spectral index associated with AGNs results in a normalization of the *ROSAT* log N–log S relation in the 2–10 keV band which lies a factor of 3 below that found by the *Ginga* $P(D)$ distribution (Stewart 1992). From Fig. 2, it is easy to see that our model does provide a quantitative explanation of the observed discrepancy. We stress that, in the 2–10 keV range, heavily absorbed type 2 Seyferts resemble steep-spectrum, faint type 1 Seyferts. Fig. 1(a) shows how the direct continuum is completely hidden from our view by a hydrogen column of $\gtrsim 10^{24}$ cm^{-2}. In this band we are only able to detect the 2 per cent scattered component, a power law without any strong absorption feature, as in the case of NGC 1068. The main distinguishing feature is the strong iron line (cf. NGC 6552: Fukazawa et al. 1994). Self-absorbed sources with columns $N_H \sim$ a few $\times 10^{23}$ cm^{-2} should, however, be easily detectable by *ASCA*.

ACKNOWLEDGMENTS

We thank R. Burg for useful discussions and comments.

REFERENCES

Antonucci R. R. J., 1993, ARA&A, 31, 473
Antonucci R. R. J., Miller J. S., 1985, ApJ, 297, 621
Awaki H., 1992, in Makino F., Nagase F., eds, *Ginga* Memorial Symposium. ISAS, Tokyo, p. 63
Awaki H., Koyama K., Inoue H., Halpern J. P., 1991, PASJ, 43, 195
Boldt E., 1987, Phys. Rep., 146, 215
Boyle B. J., 1991, Ann. NY Acad. Sci., 647, 14
Boyle B. J., Griffiths R. E., Shanks T., Stewart G. C., Georgantopoulos I., 1993, MNRAS, 260, 49
Butcher J. A. et al., 1994, MNRAS, in press
Comastri A., Setti G., Zamorani G., Elvis M., Giommi P., Wilkes B., McDowell J., 1992, 384, 62
Comastri A., Hasinger G., Setti G., Zamorani G., 1994, in Bicknell G. V., Dopita M. A., Quinn P. J., eds, ASP Conf. Ser., Proc. First Stromlo Symp.: The Physics of Active Galaxies. Astron. Soc. Pac., San Francisco, p. 143
Della Ceca R., Maccacaro T., Gioia I. M., Wolter A., Stocke J. T., 1992, ApJ, 389, 491
Fabian A. C., George I. M., Miyoshi S., Rees M. J., 1990, MNRAS, 242, 14P
Franceschini A., Martín-Mirones J. M., Danese L., De Zotti G., 1993, MNRAS, 264, 35
Fukazawa Y. et al., 1994, PASJ, in press
Gendreau K. et al., 1994, PASJ, in press
Ghisellini G., Haardt F., Matt G., 1994, MNRAS, 267, 743

Grindlay J. E., Luke M., 1990, in Gorenstein P., Zombeck P., eds, Proc. IAU Colloq. 115. Cambridge Univ. Press, Cambridge, p. 276
Hasinger G., Schmidt M., Trümper J., 1991, A&A, 246, L2
Hasinger G., Burg R., Giacconi R., Hartner G., Schmidt M., Trümper J., Zamorani G., 1993, A&A, 275, 1
Huchra J., Burg R., 1992, ApJ, 393, 90
Johnson W. N. et al., 1994, Fichtel C., Gehrels N., Norris J. P., eds, Proceedings of the Second Compton Symposium. University of Maryland, College Park, MD, p. 515
Krolik J. H., Madau P., Życki P. T., 1994, ApJ, 420, L57
Madau P., Ghisellini G., Fabian A. C., 1993, ApJ, 410, L7 (Paper I)
Madejski G. et al., 1994, ApJ, in press
Maisack M. et al., 1993, ApJ, 407, L61
Matsuoka M., Piro L., Yamauchi M., Murakami T., 1990, ApJ, 361, 440
Matt G., Fabian A. C., 1994, MNRAS, 267, 187
Miller J. S., Goodrich R. W., 1990, ApJ, 355, 456
Miller J. S., Goodrich R. W., Mathews W. G., 1991, ApJ, 378, 47
Miyaji T., Lahav O., Jahoda K., Boldt E., 1994, ApJ, in press
Morisawa K., Matsuoka M., Takahara F., Piro L., 1990, A&A, 236, 299
Morrison R., McCammon D., 1983, ApJ, 270, 119
Mulchaey J. S., Mushotzky R. F., Weaver K. A., 1992, ApJ, 390, L69
Nandra P., Pounds K. A., 1994, MNRAS, 268, 405
Osterbrock D. E., Shaw R. A., 1988, ApJ, 327, 89
Persic M., De Zotti G., Danese L., Palumbo G. G. C., Franceschini A., Boldt E. A., Marshall F. E., 1989, ApJ, 344, 125
Phillips M. M., Charles P. A., Baldwin J. A., 1983, ApJ, 266, 485
Piccinotti G., Mushotzky R. F., Boldt E. A., Holt S. S., Marshall F. E., Serlemitsos P. J., Shafer R. A., 1982, ApJ, 253, 485
Pounds K. A., Nandra K., Stewart G. C., George I. M., Fabian A. C., 1990, Nat, 344, 132
Pozdnyakov L. A., Sobol' I. M., Sunyaev R. A., 1983, Astrophys. Space Sci. Rev., Vol. 2, p. 189
Rogers R. D., Field G. B., 1991, ApJ, 370, L57
Setti G., Woltjer L., 1989, A&A, 224, L21
Shanks T., Georgantopoulos I., Stewart G. C., Pounds K. A., Boyle B. J., Griffiths R. E., 1991, Nat, 353, 315
Stewart G. C., 1992, in Barcons X., Fabian A. C., eds, The X-Ray Background. Cambridge Univ. Press, Cambridge, p. 259
Sunyaev R. A., Titarchuk L. G., 1980, A&A, 86, 121
Svensson R., 1984, MNRAS, 209, 175
Terasawa N., 1991, ApJ, 378, L11
Turner T. J., Pounds K. A., 1989, MNRAS, 240, 833
Wu X., Hamilton T., Helfand D. J., Wang Q., 1990, ApJ, 379, 564
Zdziarski A. A., Życki P. T., Krolik J. H., 1993, ApJ, 414, L81
Zitelli V., Mignoli M., Zamorani G., Marano B., Boyle B. J., 1992, MNRAS, 256, 349